High-sensitivity cryogenic temperature sensors using pressurized fiber Bragg gratings

Meng-Chou Wu* and Stanton L. DeHaven

NASA, Langley Research Center, MS 231, Hampton, Virginia, 23681-2199, USA

ABSTRACT

Cryogenic temperature sensing was studied using a pressurized fiber Bragg grating (PFBG). The PFBG was obtained by simply applying a small diametric load to a regular fiber Bragg grating (FBG), which was coated with polyimide of a thickness of 11 micrometers. The Bragg wavelength of the PFBG was measured at temperatures from 295 to 4.2 K. A pressure-induced transition occurred at 200 K during the cooling cycle. As a result the temperature sensitivity of the PFBG was found to be nonlinear but reach 24 pm/K below 200 K, more than three times the regular FBG. For the temperature change from 80 K to 10 K, the PFBG has a total Bragg wavelength shift of about 470 pm, 10 times more than the regular FBG. From room temperature to liquid helium temperature the PFBG gives a total wavelength shift of 3.78 nm, compared to the FBG of 1.51 nm. The effect of the coating thickness on the temperature sensitivity of the gratings is also discussed.

Keywords: fiber Bragg gratings, temperature sensors, cryogenic temperatures, pressurized fiber Bragg gratings

1. INTRODUCTION

Fiber Bragg gratings (FBGs) have been extensively studied for temperature and strain sensing in health monitoring systems of aerospace vehicles and other applications.[1-3] Compared with other types of sensors, FBGs have the advantages of being lightweight and flexible, and also requiring simpler wiring especially for distributed sensing systems. FBGs are also candidates for multiple parameter sensing. Several techniques have been developed for simultaneous measurements of strain and temperature.[4-6] However, they can be applied only to a finite range of temperatures. In general, strain response of FBGs is linear for a broad range of strain and independent of temperature.[7] The temperature response of FBGs is much more complicated. Although for temperatures above 273 K the temperature sensitivity of FBGs is also relatively linear, it becomes more nonlinear for the lower temperatures and much smaller for cryogenic temperatures. In addition, there are also problems of wavelength shift continuity with FBGs in the cryogenic temperature range. To ensure the FBGs have the capability of temperature sensing in the temperature range of interest: first, the temperature sensitivity needs to be increased; second, their waveforms, which are used as indicators of temperatures, have to be stable and well-defined.

It has been suggested that FBGs be embedded in or bonded to substrates to enhance their temperature sensitivity.[8,9] These substrates, e.g., poly(methyl methacrylate) (PMMA) or Teflon, have a thermal expansion greater than that of the silica fibers. Nevertheless it is also required that the thickness of the substrate should be much greater than the diameter of the fiber and the length of the substrate longer than that of the FBG. Therefore dimensions of these substrates are of the order of several millimeters to centimeters. Using these techniques, the enhancement of temperature sensitivity is significant. However, with such permanent bonding to substrates, the FBGs cannot retain flexibility of fiber anymore and are especially not suitable for distributed sensing with multiple sensors.

In the present work, we demonstrate a technique using pressurized Bragg gratings (PFBGs) for enhancing temperature sensitivity. PFBGs can be obtained by simply applying a small diametric load to regular FBGs. The fibers are normally coated with a thin layer of polymer, which has a thickness of only a few tens of micrometers. We have found a pressure-induced transition of the PFBGs occurs around 200 K and results in high temperature sensitivity for PFBGs at cryogenic

*Meng-Chou.Wu-1@nasa.gov

temperatures. The Bragg wavelengths of PFBGs are given over the range of 4.2 to 295 K, and compared to those of regular FBGs.

2. THEORY

In general a fiber Bragg grating can be characterized by its Bragg wavelength, which is the center wavelength of the light reflected from the grating. The Bragg wavelength is given as

$$\lambda_B = 2n_{eff}\Lambda, \tag{1}$$

where n_{eff} is the effective refractive index of the fiber core and Λ the grating period. For a fiber Bragg grating coated with polymer, a change in the temperature causes a change in the grating period due to thermal expansion of the fiber and also the strain, $\delta l/l$, induced by thermal expansion of the coating polymer. In addition, the refractive index of the fiber core changes because of the thermo-optic effect. As a result, the shift in the Bragg wavelength is given as

$$\delta\lambda_B / \lambda_B = \alpha_s\Delta T + (1 - p_e)\, \delta l/l + \delta n_{eff}/n_{eff}, \tag{2}$$

where α_s is the thermal expansion coefficient, and p_e the photoelastic constant, of the fiber, i.e., silica glass. The strain, $\delta l/l$, induced by thermal expansion of the coating polymer can be expressed as

$$\delta l/l = (\alpha_p - \alpha_s)\, \Delta T[\gamma E_p /(\gamma E_p + E_s)], \tag{3}$$

where α_p is the thermal expansion coefficient of the polymer, E_p and E_s are the Young's modulus of the polymer and silica glass respectively, and γ is defined as

$$\gamma \equiv A_p /A_s = [(r + t)^2 - r^2]/ r^2, \tag{4}$$

the ratio of the cross-sectional area, A_p, of the polymer with a thickness of t to the cross-sectional area, A_s, of the fiber with a radius of r. Eq. (3) can be further reduced as

$$\delta l/l = (\alpha_p - \alpha_s)\, \Delta T\eta, \tag{5}$$

where

$$\eta \equiv \gamma E_p /(\gamma E_p + E_s). \tag{6}$$

For a finite temperature change ΔT, so that both the thermal expansion coefficients and the index change are linear, Eq. (2) can be written as

$$\delta\lambda_B / \lambda_B = [\alpha_s + (1 - p_e)\, (\alpha_p - \alpha_s)\, \eta + \xi]\, \Delta T, \tag{7}$$

where $\xi = (1/n_{eff})(\partial n_{eff} / \partial T)$, is the thermo-optic coefficient of the fiber. It is of interest to note that when $t >> r$, $\gamma >> 1$ and $\eta \approx 1$ (also, in general $\alpha_p > \alpha_s$), therefore Eq. (7) is reduced to[8]

$$\delta\lambda_B / \lambda_B = [\, (1 - p_e)\, \alpha_p \, + \xi]\, \Delta T, \tag{8}$$

for the case of a fiber Bragg grating embedded in or bonded on a thick substrate of polymer. If $t = 0$, $\eta = 0$, then Eq. (7) becomes

$$\delta\lambda_B / \lambda_B = (\alpha_s + \xi)\, \Delta T, \tag{9}$$

the well-know formula for a bare fiber grating sensor.

In general , the second term of Eq. (7) gives the effect of the thickness of the coating on the temperature sensitivity of a fiber Bragg grating.

3. EXPERIMENT

A pulsed KrF-excimer laser of 248 nm and a Talbot interferometer arrangement were used to write the fiber Bragg gratings, as shown in Fig. 1. The interferometer consists of a phase mask performing as a beam splitter and a pair of mirrors for recombining the split beams to form an interference pattern. The opening of the aperture, regulating the spot size of the laser beam determines the length of the grating, typically of the order of 5 mm, and the spatial profile of the grating.[10] The Bragg wavelength written on the fiber can be adjusted by changing the relative angle of the two mirrors. This optical setup was mounted on the draw tower of NASA Langley Research Center for writing fiber Bragg gratings continuously in situ on drawn fibers. The single-mode fibers used in this study were drawn from commercially available germanium-doped preforms of high numerical apertures. The drawn fibers were coated with polyimide, which had thickness ranging from 11 to 16 micrometers, and ink-marked to show grating locations.

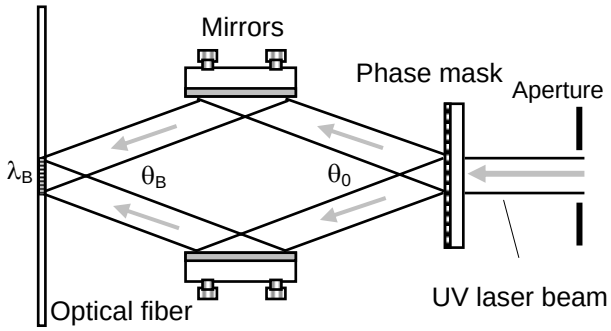

Figure 1: Schematic representation of the interferometric technique for writing fiber Bragg gratings. The Bragg wavelength λ_B is determined by the adjustable θ_B.

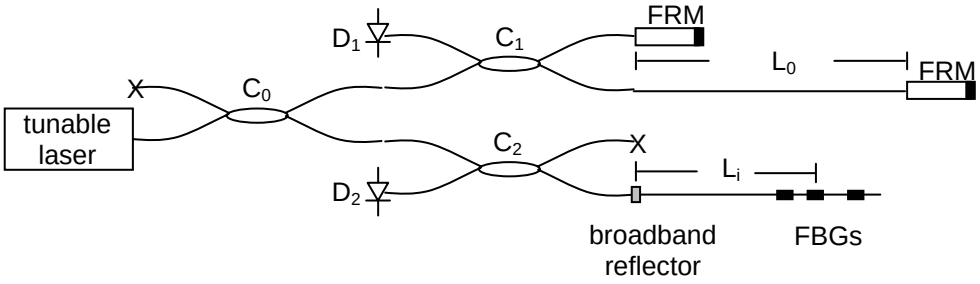

Figure 2: Schematic diagram of a frequency domain demodulation system. Items C_0, C_1, and C_2 are fiber couplers. "X" indicates that the unused port is terminated. Items D_1 and D_2 are detectors and FRMs a pair of Faraday rotation mirrors.

These low reflectivity FBGs (R smaller than a few tenths of one percent) were interrogated by using a frequency domain demodulation system[11], shown in Fig. 2. In this system, the fiber coupler C_1 and a pair of Faraday rotation mirrors (FRMs) form an in-fiber interferometer with an optical path difference of $2n_{eff}L_0$, where n_{eff} is the effective refractive index of the fiber core and L_0 the length of the reference cavity. The signals are driven by the tuning of the laser and detected at the photo-detector D_1. They are used to trigger the sampling of signal at D_2, which is the output of another in-fiber interferometer formed with the fiber coupler C_2, a broadband reflector, and a particular fiber Bragg grating at a distance of L_i. If there are a series of low reflectivity Bragg gratings written at the same wavelength on a single fiber at different locations, the reflected signals from each grating are superimposed and detected at D_2. The detected signals are further processed (fast-Fourier-transformed) to obtain the spatial spectrum of all gratings, which displays the physical profiles of the gratings at different locations. The spatial spectrum of a particular grating can then be windowed and inverse-fast-Fourier-transformed to get its own wavelength spectrum. Fig. 3(a) shows the spatial spectrum of two FBGs in a fiber with multiple gratings. The gratings have a physical length of about 5 mm and a separation distance of 10 cm. Two gray lines indicate the window of the inverse FFT for the second FBG. The wavelength spectrum of the second FBG with a center wavelength of 1551.3 nm is shown in Fig. 3(b).

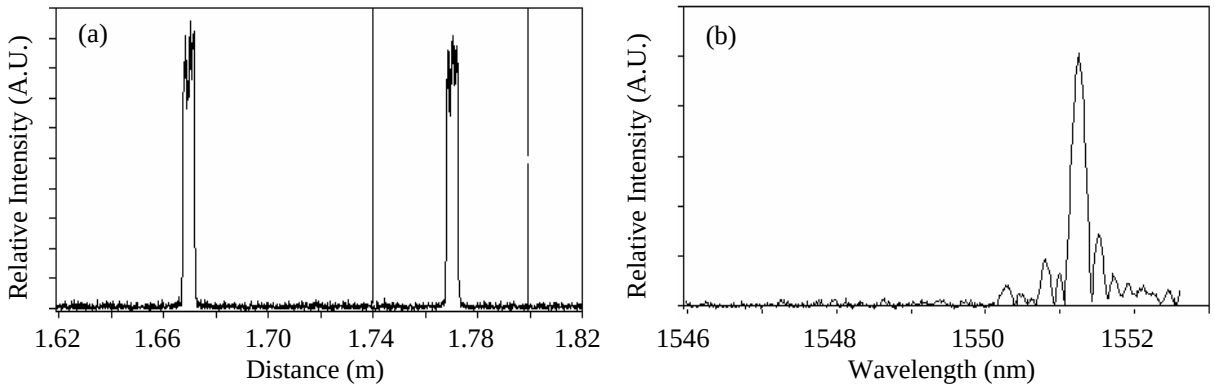

Figure 3: (a) The spatial spectrum of two FBGs with a physical length of about 5 mm. (b) The wavelength spectrum of the second FBG with a center wavelength of 1551.3 nm, resulted from the FFT windowed by the two gray lines in (a).

A cryostat of compressed helium gas was used for temperature control, ranging from 350 K to about 8 K. The optical fiber with the investigated Bragg grating was held between the cold plate of the cryogenic chamber and another copper plate with a length of about 2 cm to cover the whole Bragg grating. As shown in the Fig. 4, four screws with four identical springs are used to hold the plates and apply a small diametric load to the fiber to form a pressurized Bragg grating. A section of support fiber of equal diameter with the test fiber is added to keep the two plates parallel to each other. During the cooling process from room temperature to the lowest temperature, which took about two hours, data was taken periodically with the above frequency domain demodulation system.

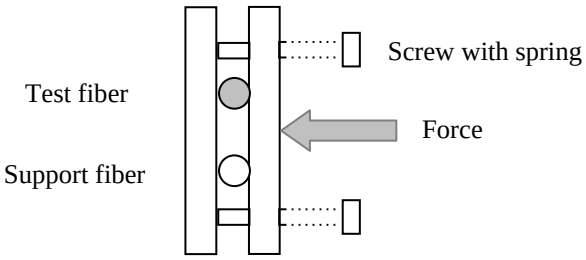

Figure 4: Schematic representation of a pressurized fiber Bragg grating. A copper plate with four screws holds the test fiber and the support fiber onto the cold plate of the cryogenic chamber. Four springs apply a diametric load to the test fiber to form a PFBG.

For comparison, fiber Bragg gratings with and without coating were also immersed directly in liquid nitrogen and liquid helium to measure their Bragg wavelength shifts.

4. RESULTS AND DISCUSSION

The measured Bragg wavelength versus temperature is shown in Fig. 5 for a regular fiber Bragg grating with polyimide coating, which has a thickness of about 11 micrometers. The fiber was only attached to the cold plate for temperature control without being pressurized. For temperatures from 295 K to 200 K, the temperature sensitivity of the regular FBG is about 8 pm/K; for temperatures ranging from 200 K to 80 K the coefficient is more nonlinear and becomes smaller as the temperature decreases; and for temperatures below 80 K the curve is almost flat, i.e., showing zero temperature sensitivity. There are also some problems of wavelength shift continuity with FBGs for the cryogenic measurements. During the cooling process, the center peak of an FBG might shift as usual but then suddenly move backwards, as shown in Fig. 5 around 90 K. This change in wavelength shift would cause an invalid measurement. Therefore, it is impractical, if not totally impossible, to use ordinary FBGs as cryogenic temperature sensors.

To obtain a PFBG, described in the section 3, the total force applied to the copper plate with 4 springs was only about 15 N. Nevertheless, to prevent a splitting of the center peak in the wavelength spectrum, no force greater than 30 N should be applied.[12] The measured Bragg wavelength as a function of temperature is shown also in Fig. 5 for the PFBG. This PFBG has the same thickness of coating as the FBG. It can be seen that the temperature sensitivity of the PFBG for temperatures from 295 K to 200 K is about 9 pm/K, not significantly greater than that of the regular FBG. However, at about 200 K, a pressure-induced transition occurs. Below 200 K the temperature coefficient of the PFBG reaches 24 pm/K, more than three times the regular FBG. Moreover, for the temperature change from 80 K to 10 K, the PFBG has a total wavelength shift of about 470 pm, 10 times more than the regular FBG does.

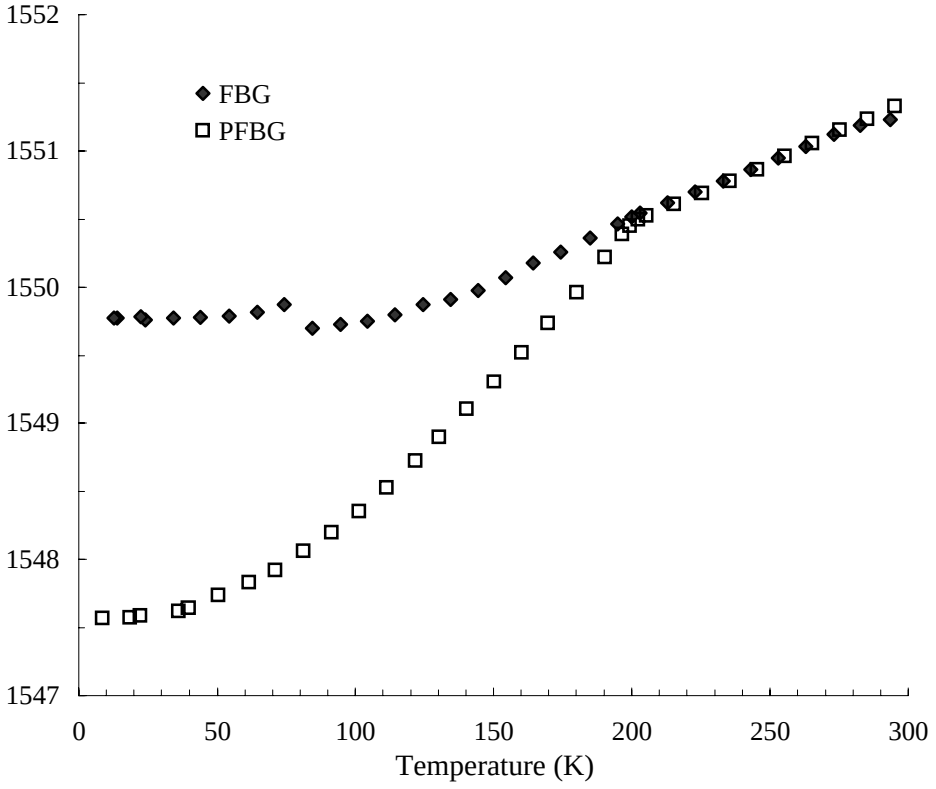

Figure 5: Bragg wavelength shifts of a FBG and a PFBG with temperature during a cooling cycle.

Table 1 shows the Bragg wavelength shifts of FBGs as they were immersed in liquid nitrogen and liquid helium directly from room temperature. The Bragg wavelength shift at the liquid nitrogen temperature is found to be $\Delta\lambda_B$ = 1.47 nm, consistent with the result from the cooling process, shown above in Fig. 5. The Bragg wavelength shift at the liquid helium temperature is $\Delta\lambda_B$ = 1.51 nm. Also shown are the results for the same fiber grating without coating, which gives $\Delta\lambda_B$ = 1. 36 nm for the liquid nitrogen temperature and $\Delta\lambda_B$ = 1.37 nm for the liquid helium. The difference between the results with and without coating is attributed to the thermal expansion of the polymer as described in the section 2, Eq. (7). For comparison, Table 1 lists the Bragg wavelength shifts of the pressurized Bragg grating for two temperatures, $\Delta\lambda_B$ (77 K) = 3.15 nm and $\Delta\lambda_B$ (8 K) = 3.78 nm, extracted from the data shown in the Fig. 5. At liquid helium temperature the difference between $\Delta\lambda_B$ with and without coating is only 0.14 nm, which would be larger for thicker coating. However, the 2.27nm difference between PFBG and FBG is much greater than the effect of the coating thickness.

Table 1. The Bragg wavelength shifts of FBGs immersed in liquid nitrogen and liquid helium, and of a PBFG at the equivalent temperatures

Fiber Bragg gratings	$\Delta\lambda_B$ (nm) (from room temperature)	
	Liquid-N_2 (77 K)	Liquid-He (4.2 K)
FBG (without coating)	1.36	1.37
FBG (with coating)	1.47	1.51
PFBG[a]	3.15	3.78

[a] from results shown in Fig. 5

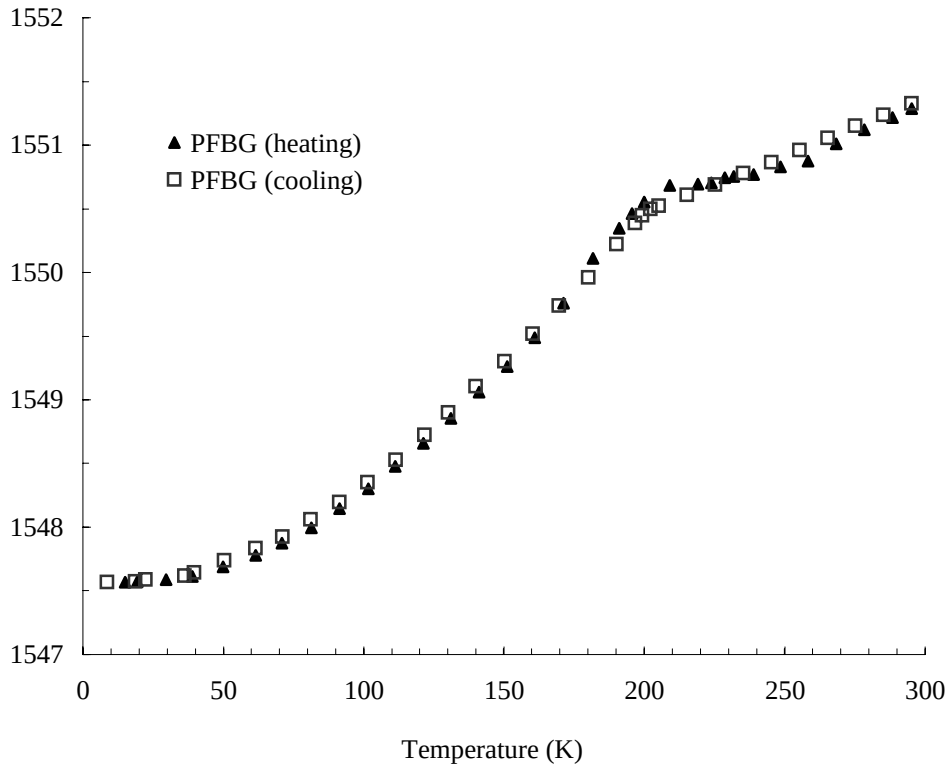

Figure 6: Bragg wavelength shifts of a PFBG with temperature during cooling and heating cycles.

Fig. 6 shows the Bragg wavelength shifts of the same PFBG during the cooling and the heating cycles. The heating cycle has a heating rate of about 4 K/min for the temperature increasing from 10 K to 295 K. At cryogenic temperatures the PFBG has the similar thermal response of heating as that of cooling, except only a very small amount of hysteresis exists. However, during the heating cycle, as the temperature passes 200 K, the transition temperature, the Bragg wavelength keeps increasing at the same rate until the temperature reaches about 210K, then decreases around 220 K and increases again at about 230 K. This overshooting indicates the relaxation time of the pressure-induced transition might be longer than the time scale, although details of the mechanism for the transition still needs further investigation.

5. CONCLUSION

We have demonstrated a technique of using pressurized fiber Bragg gratings for high sensitivity temperature sensors. PFBGs can be obtained with only a small diametric load to regular fiber Bragg gratings. Compared to a regular FBG, a PFBG has slightly greater temperature sensitivity for the temperatures from 295 K to 200 K. At 200 K, a pressure-induced transition occurs and the temperature sensitivity of the PFBG below the transition temperature reaches 24 pm/K, three times as large as that obtained with the FBG. For temperatures below 80 K, the PFBG, although showing nonlinearity, has 10 times more wavelength shift than the regular FBG does.

The PFBGs with thin polymer coating do not require any other substrates to enhance the temperature sensitivity and therefore retain the flexibility of optical fibers. The purpose of using the metal plates in this study is simply to provide the threshold stress that enables the PFBG to complete the transition. Since the required load is small, it can be obtained with a simple clamping device or cladding on fibers. The PFBGs with significantly enhanced sensitivity are apparently suitable for cryogenic temperature sensors.

ACKNOWLEDGEMENTS

The authors thank Drs. Kuen-Jenn Sun and Russell A, Wincheski for their assistance with liquid helium and immersion measurements.

REFERENCES

1. C. R. Giles, “Lightwave applications of fiber Bragg gratings,” J. Lightwave Technol. **15**, 1391-1404 (1997)
2. K. O. Hill, Y. Fujii, D. C. Johnson, and B. S. Kawasaki, “Photosensitivity in optical waveguides: application to reflection filter fabrication, “ Appl. Phys. Lett. **32**, 647-649 (1978)
3. A. D. Kersey, M. A Davis, H. J. Patrick, M. LeBlanc, K. P. Koo, C. G. Askins, M.A. Putnam, E. J. Friebele, “Fiber grating sensors,” J. Lightwave Technol. **15**, 1442-1463 (1997)
4. M. G. Xu, J.-L. Archambault, L. Reekie, and J. P. Dakin, “Discrimination between strain and temperature effects using dual-wavelength fiber grating sensors,” Electron. Lett. **31**, 823-825 (1994).
5. S. W. James, M. L. Dockney, and R. P. Tatum, “Simultaneous independent temperature and strain measurement using in-fiber Bragg grating sensors,” Electron. Lett. **32**, 1133-1134 (1996).
6. H. J. Patrick, G. M. Williams, A. D. Kersey, and J. R. Pedrazzani, “Hybrid fiber Bragg grating/long period fiber grating sensor for strain/temperature discrimination,” IEEE Photon. Technol. Lett. **8**, 1223-1225 (1996).
7. S. W. James, R. P. Tamtum, A. Twin, M. Morgan, and P. Noonan, “Strain response of fiber Bragg grating sensors at cryogenic temperatures,” Meas. Sci. Technol. **13**, 1535-1539 (2002)
8. S. Gupta, T. Mizunami, T. Yamao, and T. Shimomura, “Fiber Bragg grating cryogenic temperature sensors,” Appl. Opt. **25**, 5202-5205 (1996)
9. T. Mizunami, H. Tatehata, and H. Kawashima, “High-sensitivity cryogenic fiber-Bragg-grating temperature sensors using Teflon substrates,” Meas. Sci. Technol. **12**, 914-917 (2001)
10. M.-C. Wu and R. S. Rogowski, "Fabrication of self-apodized short-length fiber Bragg gratings," Appl. Opt. **42**, 5017-5023 (2003)
11. M. Froggatt and J. Moore, “Distributed measurement of static strain in an optical fiber with multiple Bragg gratings at nominally equal wavelengths,” Appl. Opt. **37**, 1741-1746 (1998)
12. R. B. Wagreich, W. A. Atia, H. Singh, and J. S. Sirkis, “Effects of diametric load on fiber Bragg gratings fabricated in low birefringent fiber,” Electron. Lett. **32**, 1223-1224 (1996)